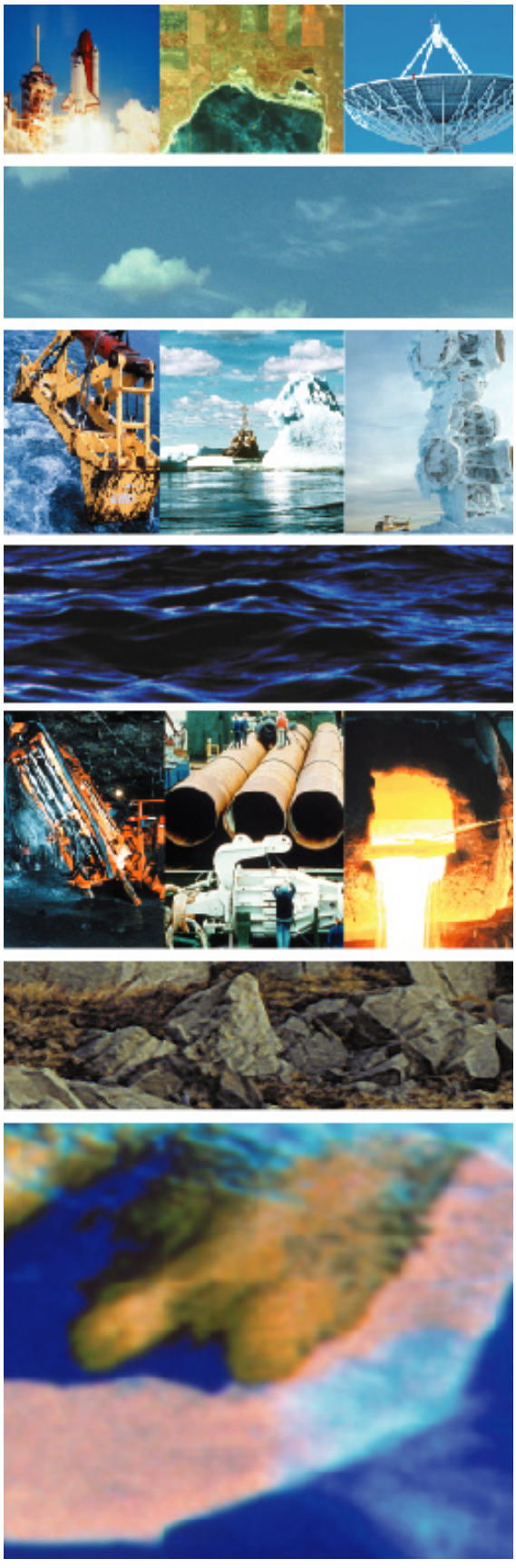

3D Finite Element Analysis of Pipe-Soil Interaction – Effects of Groundwater

Final Report

C-CORE Report R-02-029-076

February 2003

This page left blank intentionally

3D Finite Element Analysis of Pipe-Soil Interaction – Effects of Groundwater

Final Report

Prepared for:
Minerals Management Service

Prepared by:
C-CORE

C-CORE Report:
R-02-029-076
February 2003

C-CORE
Captain Robert A. Bartlett Building
Morrissey Road
St. John's, NL
Canada A1B 3X5

T: (709) 737-8354
F: (709) 737-4706

info@c-core.ca
www.c-core.ca

The correct citation for this report is:

C-CORE (2002) 3D finite element analysis of pipe-soil interaction – effects of groundwater: Final Report prepared for Minerals Management Service, C-CORE Report R-02-029-076, February 2003.

Project Team:

Radu Popescu	Memorial University of Newfoundland
Arash Nobahar	C-CORE

EXECUTIVE SUMMARY

This work is an extension of the study on 3D Finite Element Analysis of Pipe/Soil Interaction (Popescu et al. 2001), and is aimed at analysing the effects of groundwater on the soil-pipe interaction forces, for various loading conditions, and assuming either drained or undrained conditions.

Back analyses of large scale tests of lateral loading of a rigid pipe in dry and saturated sand are used to infer the changes in the shear strength of sands induced by soil saturation. Besides changes in frictional strength induced by reduction of effective confining stresses, it is found that soil saturation also affects the apparent cohesion. Those findings are used for simulating several situations analysed in the original study, and obtaining the force-displacement relations for saturated conditions.

A theoretical study is performed to infer the effects of soil saturation on pipe-soil interaction forces for pipes buried in clay. A relation accounting for changes in the failure mechanism with undrained shear strength is introduced for the case of lateral loading, and a method for estimating the interaction forces for pipes buried in saturated clays and subjected to complex loading is proposed.

TABLE OF CONTENTS

LIST OF FIGURES

LIST OF TABLES

1 INTRODUCTION

A previous 3D Finite Element Analysis of Pipe/Soil Interaction (Popescu et al. 2001) involved various situations of pipes buried in dry sand and unsaturated clay, under various loading conditions. The current research is a continuation of that study, and is aimed at analysing the effects of soil saturation on the soil-pipe interaction forces, for various loading conditions and soil materials analysed by Popescu et al. (2001), and assuming either perfectly drained or perfectly undrained conditions. Owing to significant differences between behaviour of sands and clays subjected to large deformations, the effects of saturation are analysed separately for the two types of soil materials.

1.1 Pipe Loaded in Sand under Drained Conditions

When loaded in drained conditions, the shear strength of sands is mostly provided by friction between soil particles. Frictional forces are directly dependent on the effective confining stress. When submerging a soil material, the effect of saturation is to reduce the shear strength due to reduction of the effective stresses.

In conducting this study, we have benefited from the results of large scale tests of lateral loading of a rigid pipe in dry and saturated sand performed at C-CORE and sponsored by MMS (Hurley and Phillips 1999). While a significant reduction of interaction forces due to saturation has been recorded in those tests (about 60% in the peak forces and about 40% in the residual forces), there were some results – such as the pipe displacement to the peak forces in a force-displacement plot – that could not be entirely explained by the reduction in effective stress due to submersion.

From previous studies it was concluded that, for dense sands at low confining stress, apparent cohesion due to particle interlocking may also play a role in the shear strength. A thorough numerical study based on the results of MMS tests and presented in Section 2 revealed other effects of saturation on the shear strength parameters of dense sands. The study was somehow complicated by the fact that the two MMS tests had been performed using sands with two different relative densities. This fact required some additional assumptions in assessing the effects of saturation on apparent cohesion. The results of that study are used in Section 3 to estimate the effects of soil saturation on pipe-soil interaction forces for several cases of pipes buried in sand that had been analysed by (Popescu et al. 2001).

1.2 Pipe Loaded in Clay under Undrained Conditions

Saturated clays have lower undrained shear strength than the corresponding unsaturated materials, due to the reduction in matrix suction with increasing degree of saturation. No comparative experimental studies were available for pipes buried in unsaturated and saturated clays. Moreover, none of the situations analysed by Popescu et al. (2001) and involving pipes buried in clay refer to a specific clay material or site and, therefore, the assumed undrained shear strength of those clay materials was not related to a specific type of clay, water content, or degree of saturation. Therefore, it was not possible to estimate the interaction forces for submerged pipelines corresponding to the cases presented by Popescu et al. (2001). A theoretical study involving a rigid pipe laterally loaded in various undrained clay materials was performed to assess the effects of changes in undrained shear strength (that could be produced by changes in the water content) on the soil failure mechanism and pipe-soil interaction forces. Based on the results of that study, a method is presented in Section 4 for estimating the effects of saturation on pipe-soil interaction forces for undrained clays. Special attention was given to the effects of changes in undrained shear strength on interaction diagrams for pipes buried in clay and subjected to combined bending moment and axial compression.

2 BACK ANALYSIS OF MMS TESTS

Back-analysis of lateral loading of a rigid buried pipe at C-CORE (Hurley and Phillips, 1999) were performed for two tests, MMS01 and MMS02R To better understand and quantify the effects of soil saturation on pipe-soil interaction. The two tests are summarized in Table 1. Test MMS 01 was conducted in dry sand while MMS02R was conducted in submerged conditions. Test MMS02R more closely simulated offshore conditions and a comparison of tests MMS01 and MMS02R should improve the understanding of the effects of submerged testbed conditions on the force-displacement response of a buried offshore pipeline. These tests provided the two-dimensional force-displacement (p-y) response of the pipe. In these two tests, a rigid pipe with a diameter of 0.2 m was displaced laterally by 0.1 m.

2.1 Finite Element Model

Two-dimensional, plane strain back analyses of the two large-scale MMS tests were performed using the finite element code ABAQUS/Standard (Hibbitt et al., 1998a). ABAQUS is a general purpose program for the static and transient response of two and three-dimensional systems, and offers standard options, or can be customized to address many of the challenges involved in a pipe-soil interaction study, such as: (1) 3D soil-structure interaction using complex finite-strain constitutive models, (2) coupled field equations capabilities for two-phase media, (3) contact analysis capabilities for simulating the soil-pipe interface, and (4) nonlinear shell elements that have been proven to reproduce buckling and wrinkling of pipelines. ABAQUS/Standard is widely available and is very well-documented. The program has been used in the past at C-CORE for 2D and 3D finite element analyses of pipe-soil interaction involving large relative deformations, and has been validated based on results of full-scale tests (Popescu, 1999; Popescu et al., 2001).

2.1.1 Finite Element Mesh

Two finite element meshes were built using the experimental set-up for tests MMS01 and MMS02R (Figure 1 and Figure 2). The soil was discretized using quadratic finite elements with 8 nodes and reduced integration (i.e., element CPE8R in ABAQUS), as shown in Figure 3. Three-node quadratic beam structural elements (B22) were used to simulate the rigid pipeline in a cross-section. These second order elements were proven to yield higher accuracy than linear elements at the same computational effort (Popescu 1999).

The contact surface approach implemented in ABAQUS/Standard that allows for the separation and sliding of finite amplitude and arbitrary relative rotation of the contact surfaces, was used to simulate the pipe-soil interface. The contact was assumed frictional, with Coulomb friction. The shear stress between the surfaces in contact was limited by a maximum value $t_{max} = \mu p$, where p is the normal effective contact pressure, and μ is the friction coefficient. A value of $\tan(0.6\phi)$ was taken for μ, where ϕ is soil friction angle (Trautmann and O'Rourke, 1983; ASCE, 1984). In both tests, a rigid pipe with diameter of 203 mm and length of 2996 mm was used.

2.1.2 Material Properties

Sand materials were modelled using an extended Mohr Coulomb model with friction and apparent cohesion. The soil properties in tests MMS01 and MMS02R are different (see Table 1). Test MMS01 has a soil with a relative density of 95%. Due to the similarity between this soil and the dense soil analysed by Nobahar et al. (2000) and Popescu et al. (2001), the hardening/softening parameters were estimated from hardening/softening rules derived in the aforementioned studies based on results of direct shear box laboratory soil tests. It was found, however, that the soil used in test MMS01 had somewhat different grain-size distribution and a higher friction angle than those of the dense sand analysed by Nobahar et al. (2000) and Popescu et al. (2001). Moreover, the sand in the direct shear box tests had an apparent cohesion as high as 20 kPa at peak, while no apparent cohesion was reported for the MMS01 soil. To account for the differences between the two soils, it was decided that the apparent cohesion be adjusted for the soil in test MMS01 as discussed hereafter.

A friction angle of 53 degrees was reported for soil in the MMS tests. Friction angles larger than 44-45 degrees are often not trusted and can be attributed to apparent cohesion and interlocking (see Schmertmann, 1978 for ranges of soil friction angle). Therefore, the friction angle was limited to a value of 44 degrees, and an equivalent cohesion was estimated for the soil to compensate the reduced friction angle at the desired soil pressure level. Figure 4 shows predicted contours of mean effective stress at the peak interaction force. The mean effective stress in front of the pipe, where maximum shear stress is mobilized, has a value of about 70 kPa. In the p-q plane (q is the Mises stress) the following relations are valid (Craig, 1992):

$$\tan\alpha = \sin\phi \qquad \text{Eq. 1}$$

$$c = \frac{\alpha}{\cos\phi}$$

where a and a are the friction angle and cohesion in the p-q plane. From the condition to obtain the same shear strength at a mean effective stress of 70 kPa for a friction angle, $\phi=44^o$, which corresponds to $\alpha=34.8^o$. An apparent cohesion $a = 7.23\ kPa$ in the p-q plane, was estimated (Figure 5). This corresponds to a cohesion $c = 10\ kPa$ (from Eq. 1). For plane strain loading condition (Hibbitt et al., 1998b), the resulting value for cohesion would be 10.1 kPa. In conclusion, the following soil properties were used for sand with relative density, D_r=95%:

- Peak friction angle, $f_{max} = 44^o$ and residual friction angle $f_{residual} = 35^o$
- Peak cohesion, $c_{max} = 10$ kPa, $c_{min} = 5$ kPa (imposed by the particularities of the soil constitutive model – see Popescu et al. 1999).
- The dilation angle, y, was estimated using Rowe's (1962) relation:

$$\sin y = \frac{\sin f - \sin f_{cv}}{1 - \sin f \sin f_{cv}} \qquad \text{Eq. 2}$$

- Deformation modulus, $E = 9000$ kPa (Popescu et al. 2001)
- Poisson's ratio, $n = 0.33$
- Friction coefficient at soil/pipe interface, $m = tan(0.6f) = 0.5$ – see Trautmann and O'Rourke (1983) and ASCE(1984)
- Soil unit weight see Table 1
- Hardening/softening rule as shown in Figure 6a

The sand used in MMS02R test had a relative density D_r=66% (Table 1). The peak friction angle was adjusted based on the study reported by Schmertmann (1978). A peak friction angle $f_{max} = 41^0$ was interpolated for this soil with relative density D_r=66%, assuming a friction angle of 44^0 and 35^0 for sands with relative densities of 95% and 10%, respectively (see Popescu et al. 2001 for the characteristics of very loose sand). Also due to saturation and presence of water (lubricating effects), a smaller apparent cohesion was expected. Therefore a minimum cohesion, c=2.5 kPa, imposed by the specific soil constitutive model (Popescu et al. 1999) was used in the analysis. Young's modulus was reduced based on the mean effective stress level in front of the pipe, as suggested by Lambe and Whitman (1969) and Richard et al. (1970),

$$E \propto s_o^{0.5} \qquad \text{Eq. 3}$$

The following soil properties were used in the back-analysis of test MMS02R:

- Peak friction angle, $f_{max} = 41^o$ for relative density of 66% and, $f_{residual} = 35^o$
- Constant cohesion, $c = 2.5$ kPa
- Dilation as suggested by Rowe (1962) – see Eq. 2
- Deformation modulus, $E = 6650$ kPa
- Poisson's ratio, $n = 0.33$
- Friction coefficient at soil/pipe interface, $m = tan(0.6f) = 0.4$ – see Trautmann and O'Rouke (1983) and ASCE(1984)
- Soil unit weight see Table 1
- Hardening/softening rule interpolated for a relative density of 66% as shown in Figure 6b

The soil constitutive model parameters were estimated on the basis of results of laboratory soil tests, engineering judgment, and previous experience. The objective had been to obtain a set of soil parameters of the soil used in the laboratory tests of the MMS projects and a set of assumptions compatible to engineering principles, and at the same time to accurately reproduce the force-displacement relations recorded in the experiments.

2.2 Pipe in Dry and Saturated Sand

Figure 7 shows the experimental results from tests MMS01 and MMS02R in terms of force-displacement relations. The experimentally recorded results are plotted in terms of sum of forces recorded by the master and slave cell loads for the whole length of the pipe.

2.2.1 Pipe in dense dry sand – test MMS01

Figure 8 shows the finite element predictions and experimental results for test MMS01 (dry sand) of lateral loading of a rigid buried pipe in terms of force-displacement per unit length (1 meter) of pipe. The finite element predictions match the recorded results well. The differences between numerical predictions and experimental results are in the same order of magnitude with the differences between recorded results from slave and master cells. Figure 9 shows predicted contours of plastic shear strain in the soil at pipe displacements of 10 mm and 20 mm, indicating that the predicted failure mechanism of dense sand subjected to lateral loading of pipe is general shear failure. A similar failure

mechanism was observed in other large-scale tests of lateral loading of a rigid pipe in dry dense sand (e.g. Paulin et al. 1998) and was predicted by Popescu et al. (2001).

2.2.2 Pipe in saturated medium dense sand – test MMS02R

Figure 10 shows the finite element predictions and experimentally recorded results for test MMS02R of lateral loading of a rigid buried pipe in terms of force-displacement per unit length. There is a good match between the finite element predictions and experimental results. Figure 11 shows predicted plastic shear strains in soil at pipe displacement of 10 mm indicating that the predicted failure mechanism of medium dense sand subjected to lateral loading of pipe is also a general shear failure, similar to that predicted for the dry dense sand.

3 EFFECTS OF GROUNDWATER ON INTERACTION FORCES FOR PIPES BURIED IN SATURATED SAND – DRAINED BEHAVIOUR

From the back-analysis of the two MMS tests, it was concluded that there should be a significant drop in apparent cohesion between tests MMS01 (dry soil) and MMS02R (saturated soil). The question is what percentage of this drop can be attributed to presence of water and what percentage to the change in the relative density – MMS01 had a relative density of about 95% in comparison to 66% for MMS02R (Table 1). Popescu et al. 2001 found that the loose sand in their study had no apparent cohesion. However, they used a minimum value of cohesion imposed by the particularities of the soil constitutive model. Assuming a linear variation of apparent cohesion from very dense sand to very loose sand, the apparent cohesion is estimated as shown in Figure 12a for a dry soil with relative density of 66%.

The best fit in the back-analysis of test MMS02R was obtained using minimum cohesion. With the above assumptions (shown in Figure 12a), about half of the reduction in apparent cohesion can be attributed to the effects of soil particle wetting, and the other half to the reduction in relative density from 95% to 66% between tests MMS01 and MMS02R.

Using the same assumptions for the large-scale tests of lateral loading of a rigid pipe buried in sand (C-CORE 1996) analysed by Popescu et al. (2001), the soil parameters were obtained as shown in Figure 12b. Those two tests were re-analysed, assuming saturated conditions for the sand. The following changes in soil parameters with respect to the ones used by Popescu et al. (2001) were made for the saturated sands:

- Dense sand: use buoyant unit weight and apparent cohesion as shown by the yellow line in Figure 12b.
- Loose sand: use buoyant unit weight

The predicted force-displacement relations for saturated sand are compared to the ones predicted by Popescu et al. (2001) for dry sand in Figure 13. A reduction in peak forces due to saturation of about 45% is predicted for dense sand (Figure 13a), were both the frictional strength and the apparent cohesion were assumed to be affected by soil saturation. The reduction in soil-pipe interaction forces was about 25% for loose sand.

Test GSC01 – moment loading of a flexible pipe in dense sand (Hurley et al., 1998a) – was also reanalysed for saturated conditions. The results for one case – constant Young's modulus – are compared in Figure 14 with the test experimental results and the finite element predictions for dry sand. For this case, it was predicted that soil saturation

induced a reduction in the soil-pipe interaction forces of about 25%, with respect to the dry sand situation (compare the continuous and dashed blue lines in Figure 14). The effects of soil saturation on soil-pipe interaction forces for the case of moment loading (25% reduction) were significantly lower than for the case of lateral loading (45% reduction). This difference is believed to be due to the fact that, in the case of moment loading, the pipe material itself contributes to supporting the external loads.

4 EFFECTS OF GROUNDWATER ON INTERACTION FORCES FOR PIPES BURIED IN CLAY – UNDRAINED BEHAVIOUR

4.1 Introduction

The presence of water in clayey soils decreases both the undrained shear strength and the effective unit weight. Unlike in drained conditions, buoyancy forces do not affect the shear strength of the undrained clay. They only affect the effective weight of the failing wedge of soil, in the case of general shear failure, and are deemed to have little influence on pipe-soil interaction. The main difference consists in the value of undrained shear strength that is dependent on the effective stresses controlled by matrix suction. For example, experimental results of full scale tests of lateral loading of a rigid pipe in uniform clay (e.g. Paulin et al. 1998) show an increase of about 60% in the ultimate interaction forces, P_{ult}, due to a reduction of water content from about 37% to about 33%. This result can only be used as a qualitative indication, since the actual changes in shear strength depend on the type of clay and the degrees of saturation. Finally, given the large differences in behaviour between different types of clay, one can infer the changes in interaction forces due to saturation only if values of the undrained shear strength of the saturated soil are available.

4.2 Effects of Soil Stiffness on Normalized Lateral Loads

None of the situations analysed by Popescu et al. (2001) involving pipes buried in clay refer to a specific clay or site and, therefore, the assumed undrained shear strength of those clays was not related to a specific type of clay, water content, or degree of saturation. Therefore, it is not possible at this time to provide any quantitative estimate of the interaction forces for submerged pipelines corresponding to the cases presented by Popescu et al. (2001). Once the undrained shear strength profile of the saturated soil is known, the soil-pipe interaction forces can be calculated using the finite element method, as shown by Popescu et al. (2001). Another way is to use current practice guidelines. The remainder of this section discusses this second approach.

In the current design practice, the relation between pipe relative displacements and interaction forces is related to the non-linear soil response through simple non-linear elastic relations. The guidelines currently used in North America (ASCE 1984) suggest a hyperbolic relation between the lateral load per unit length of pipeline, P, and the lateral relative displacement between pipeline and soil, Y. This is expressed in terms of the

ultimate lateral soil load per meter of pipe, P_{ult}, and displacement to ultimate load, Y_{ult}. For example, the ultimate lateral soil load for clays is expressed as:

$$P_{ult} = N_{ch}\, c_u\, D \qquad \text{Eq. 4}$$

where N_{ch} is the bearing capacity factor for vertical strip footings horizontally loaded, D is the external pipe diameter, and c_u the undrained shear strength of the soil. Various analytical models used to estimate P_{ult} as well as experimental data show substantial differences, leading to predictions differing by as much as 240% (Rowe and Davis 1982, Trautmann and O'Rourke 1985).

The ASCE (1984) guidelines adopted Hansen's (1961) model for vertical piles subjected to lateral loading. The bearing capacity factor is given as a function of the embedment ratio, H/D. Another widely used empirical relation was proposed by Rowe and Davis (1982), in which was based on results of elastic-plastic finite element analyses of vertically oriented anchors. They acknowledged the presence of different failure mechanisms as a function of cover depth and soil strength. In their formulation, the interaction force is expressed explicitly as a function of both the overburden pressure and a coefficient for the effects of overburden pressure that varies with embedment ratio. These two relations, by Hansen (1961) and by Rowe and Davis (1982), will be discussed hereafter and compared with finite element analysis results.

Figure 15 and Figure 16 present some of the results of a study on the effects of soil undrained shear strength on lateral interaction forces. A buried pipe with an embedment ratio H/D=3, where H is the depth to the springline and D is the pipe diameter, is translated laterally under undrained conditions in two different soils: a very soft clay, with undrained shear strength c_u=10 kPa, and a stiff clay, with c_u=100 kPa. Figure 15 presents the predicted displacements in soil at pipe displacements d=D. The stiff clay exhibits shear failure, while the soft clay "flows" around the pipe, in a pattern labelled by Rowe and Davis (1982) as "stick condition".

The predicted normalized lateral interaction forces are usually expressed as:

$$N = P / (c_u\, D) \qquad \text{Eq. 5}$$

where P is the interaction force per 1 m of pipe, as presented in Figure 16 for four different values of the soil shear strength. They are compared with the ultimate forces, P_{ult}, calculated according to the ASCE (1984) guidelines (Hansen's 1961 formula) and to the limiting expressions suggested by Rowe and Davis (1982) for very stiff clays ("non-stick" condition) and very soft soils ("stick" condition). These ultimate force values are

shown by horizontal lines in Figure 16. The numerical results are in close agreement with Rowe and Davis' results, showing a clear increase in normalized interaction forces with decreasing undrained shear strength. To obtain similar normalized interaction forces for all cases, modification of Eq. 5 is suggested as follows (Popescu et al. 2002):

$$P_{ult} / (c_u D) = N_{ch} + \alpha / c_u \qquad \text{Eq. 6}$$

where α is a factor including the effects of soil weight and type of soil failure mechanism. Eq. 6 can be used for inferring the interaction forces for lateral loading of a rigid pipe in clay, given the undrained shear strength of the soil. The bearing capacity factor, N_{ch}, can be estimated based on Hansen's (1961) formula, as recommended by the ASCE (1984) guidelines. For the case analysed here (soil total unit weight γ = 18 kN/m^3 and embedment ratio H/D = 3) an α value of about 45 kPa is predicted. More investigations are necessary for estimating if and how the parameter α depends on the pipe embedment ratio and on the soil unit weight.

4.3 Analysis of Complex Loading Situations

Eq. 6 presented in the previous section is only valid for lateral loading of buried rigid pipes. In other loading situations, such as moment loading, the pipe material itself contributes to supporting the external loads, and the effects of changes in undrained shear strength of soil on soil-pipe interaction forces are diminished. The results obtained for sands that were discussed in Chapter 3 of this study and presented in Figure 13 (for lateral loading) and Figure 14 (for moment loading) are relevant in this respect.

Using the results of the study presented in Section 4.2, a method is suggested next for inferring pipe-soil interaction forces for submerged conditions, based on the results of finite element analyses of pipes buried in clay and subjected to complex loading presented by Popescu et al. (2001). The procedure outlined in this section does not account for changes in the total unit weight of soil due to saturation, as more research is necessary to infer this type of dependence. The necessary data are:

- undrained shear strength of the non-saturated soil (c_u^{NS})
- ultimate force per meter of pipe, P_{ult}^{NS}, for lateral loading obtained using c_u^{NS}
- undrained shear strength of the saturated soil (c_u^{S})

The proposed procedure consists of two steps:

1) estimate the bearing capacity factor N_{ch} from Eq. 6 as:

$$N_{ch} = \frac{P_{ult}^{NS}}{c_u^{NS} D} - \frac{a}{c_u^{NS}} \qquad \text{Eq. 7}$$

2) using the undrained shear strength of the saturated soil, c_u^S, calculate the ultimate interaction force P_{ult}^S for the submerged pipe as:

$$P_{ult}^S = P_{ult}^{NS} r - \alpha D (1 - r) \qquad \text{Eq. 8}$$

where $r = c_u^S / c_u^{NS}$.

Presented next in an example on how to apply the above method to the study presented in Chapter 9 of Popescu et al. (2001), referring to interaction diagrams for buried pipelines subjected to combined bending moment and axial force loading. As shown in Section 9.4.3 and Figures 9.19 and 9.20 of that report, the effect of the presence of the soil is to increase the bending moment capacity of buried pipes, as compared to pipes loaded in air. Until more studies become available, it is suggested that a change (reduction) in the undrained shear strength (from c_u^{NS} to c_u^S) due to soil saturation be reflected by a corresponding reduction of the moment capacity. With the notations in Figure 17, for a given axial force, N_i, the increase in bending moment capacity of a pipe buried in saturated soil could be estimated as:

$$M_i^S - M_i^A = (M_i^{NS} - M_i^A) (P_{ult}^S c_u^S) / (P_{ult}^{NS} c_u^{NS}) \qquad \text{Eq. 9}$$

where M_i^S, M_i^{NS} and M_i^A are bending moment capacities (applied loads) in a saturated clay, non-saturated clay and in air, respectively, corresponding to the axial force N_i. The dashed line in Figure 17 represents the estimated interaction diagram (applied loads) corresponding to a reduction of the undrained shear strength from c_u^{NS}=50 kPa to c_u^S=10 kPa due to soil saturation. For this mathematical exercise, the ultimate forces have been obtained from the study in Section 4.2 and Figure 16. The ratio $(P_{ult}^S c_u^S)/(P_{ult}^{NS} c_u^{NS})$ in Eq. 9 was approximately 0.3.

5 CONCLUSIONS

This work was aimed at analysing the effects of soil saturation on the soil-pipe interaction forces, for various loading conditions and soil materials analysed by Popescu et al. (2001), and assuming either perfectly drained or perfectly undrained conditions. Owing to differences in constitutive behaviour, sands and clays were analysed separately.

- For pipes buried in sand, it was found from back analyses of large-scale tests of lateral loading of a rigid pipe in dry and saturated sand that, besides changes in frictional strength induced by reduction in effective confining stresses, soil saturation also affects the apparent cohesion.

Those findings were used for simulating several situations analysed in the original study, and obtaining the force-displacement relations for saturated conditions.

- The effects of soil saturation on interaction forces were found to be dependent on the loading mechanism.

None of the situations analysed by Popescu et al. (2001) and involving pipes buried in clay referred to a specific clay material or site and, therefore, the assumed undrained shear strength of those clay materials was not related to a specific type of clay, water content, or degree of saturation. Therefore, it was not possible to provide any quantitative estimate of the interaction forces for submerged pipelines corresponding to the cases presented in the original study.

A theoretical study involving a rigid pipe laterally loaded in various clay materials was performed to assess the effects of changes in undrained shear strength (that could be produced by changes in the water content) on the soil failure mechanism and pipe-soil interaction forces for the case of lateral loading.

- The study confirmed earlier results by Rowe and Davis (1982) related to changes in soil failure mechanism as a function of the undrained shear strength of clay. A quantitative relation to account for those changes was proposed. Based on the results of that study, a method was presented for estimating the effects of saturation on pipe-soil interaction forces in undrained complex loading conditions.

6 REFERENCES

ASCE (1984). Guidelines for the seismic design of oil and gas pipeline systems. Committee on Gas and Liquid Fuel Lifelines, Technical Council on Lifeline Earthquake Engineering, ASCE, New York.

C-CORE, (1996). Full scale pipe/soil interaction study; lateral loading in sand. C-CORE Publication 96-C36.

Craig, R.F. (1992). Soil mechanics. Chapman & Hall, London, Fifth edition, 427 pages.

Hansen, J.B. (1961). The ultimate resistance of rigid piles against transversal forces. Bulletin 12, Danish Geotech. Inst., Copenhagen, pp.5-9.

Hibbitt, Karlsson & Sorensen, Inc., (1998a). ABAQUS User Manual, version 5.8.

Hibbitt, Karlsson & Sorensen, Inc., (1998b). ABAQUS Theory Manual, version 5.8.

Hurley, S. and Phillips, R. (1999). Large scale modelling of pipeline/soil interaction under lateral loading - Final Report. Contract Report for Minerals Management Service, U.S. Department of the Interior, C-CORE Publication 99-C25.

Hurley, S., Zhu, F., Phillips, R. and Paulin, M. J. (1998a). Large scale modelling of soil/pipe interaction under moment loading, Test GSC 01 data report. Contract Report for Terrain Sciences Division. Geological Survey of Canada, C-CORE Publication 98-C20.

Hurley, S., Zhu, F., Phillips, R. and Paulin, M. J. (1998b). Large scale modelling of soil/pipe interaction under moment loading, Test GSC 02 data report. Contract Report for Terrain Sciences Division. Geological Survey of Canada, C-CORE Publication 98-C21.

Lambe, T.W., and Whitman, R. (1969). Soil mechanics in engineering practice. Chichester/New York, John Wiley & Sons.

Nobahar, A., Popescu, R., and Konuk, I. (2000). Estimating progressive mobilization of soil strength. Proceedings of 53rd Canadian Geotechnical Conference, pp. 1311-1317.

Paulin, M.J., Phillips, R., Clark, J.I., Trigg, A. and Konuk, I. (1998). A full-scale investigation into pipeline/soil interaction. Proc. International Pipeline Conf., ASME, p779-788, Calgary, AB.

Popescu, R. (1999). Finite element analysis of pipe/soil interaction phase 1 - two-dimensional plane strain analyses. Contract Report for the Geological Survey of Canada. C-CORE Publication 99-C23.

Popescu, R., Phillips, R., Deacu, D. and Konuk, I. (1999). Physical and numerical analysis of pipe-soil interaction. Proc. 52nd Canadian Geotechnical Conference, Regina, Sask., pp. 437-444.

Popescu, R., Guo, P. and Nobahar, A. (2001). 3D finite element analysis of pipe/soil interaction. Final Report for Geological Survey of Canada, Chevron Corp. and Petro Canada, and the Minerals Management Service, C-CORE Contract Report 01-C8, 174 pages.

Popescu, R., Konuk, I., Guo, P. and Nobahar, A. (2002). Some aspects in numerical analysis of pipe/soil interaction. Proc. 2nd Canadian Spec. Conf. on Computer Appl. in Geotechnique. Winnipeg, 2002, pp. 290-297.

Rowe, P.W., 1962. The stress-dilatancy relation for static equilibrium of an assembly of particles in contact. Proc. of Royal. Society of London, 269(Series A), pp. 500-527.

Rowe, R.K. and Davis, E.H. (1982). The behaviour of anchor plates in clay. *Geotechnique*, 32(1):9-23.

Richard, R.E., Woods, R.D. and Hall, J.R., (1970). Vibration of soils and foundations. Prentice-Hall, N.J.

Schmertmann, J.H. (1978). Guidelines for cone penetration test performance and design. Report FHWA-TS-78-209, U.S. Department of Transportation, Washington, 729 pages.

Trautmann, C.H., and O'Rourke, T.D. (1983). Behaviour of pipe in dry sand under lateral and uplift loading. Geotechnical Engineering Report 83-6, Cornell University, NY, USA.

Trautmann, C.H. and O'Rourke, T.D. (1985). Lateral force-displacement response of buried pipe. Journ. Geotech. Eng., 111(9):1077-1092.

Table 1 Details of two full scale experiments performed at C-CORE for MMS (Hurley and Phillips 1999)

	Soil Condition	Sand Density (kg/m^3)	Dry Unit Weight (kN/m^3)	Relative density, RD	Peak Load (kN)	Peak Load (kN/m)	Disp. To Peak Load (mm)	Spring-line Depth (m)	Mean Effective Stress at Springline (kPa)
MMS 01	Dry	1984	19.4	94.3%	97.8	32.6	11.3	0.508	9.89
MMS 02R	Submerged	1864	18.3	66.1%	37	12.3	5.5	0.476	5.4

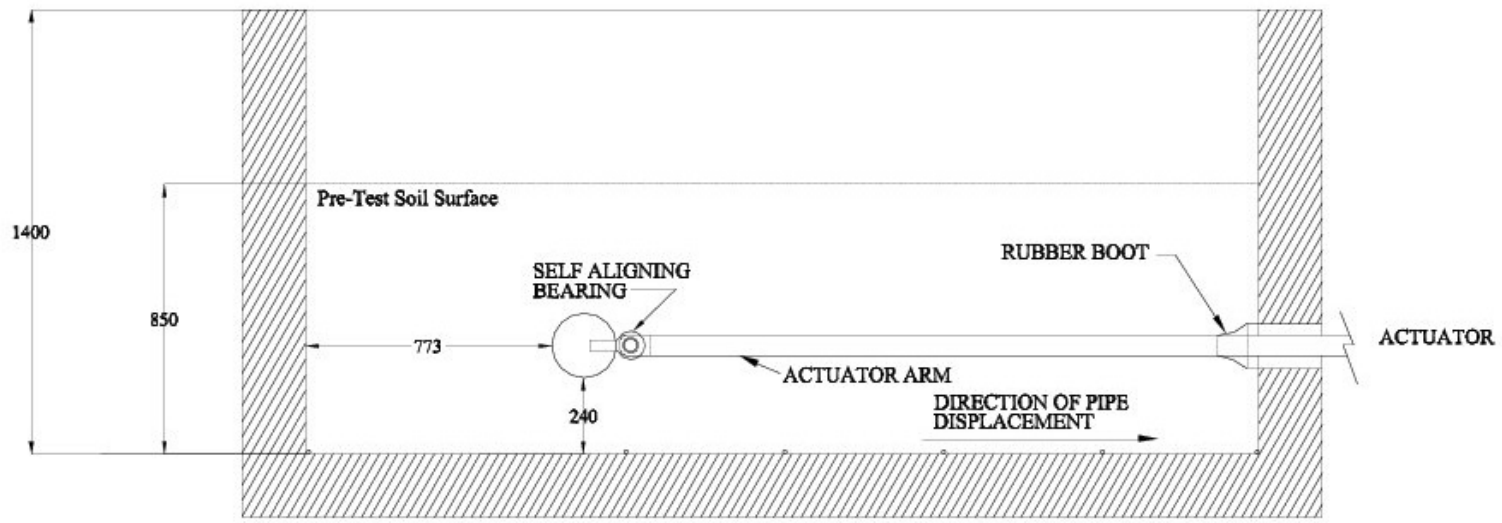

Figure 1 Experimental set-up of test MMS01 – cross-section

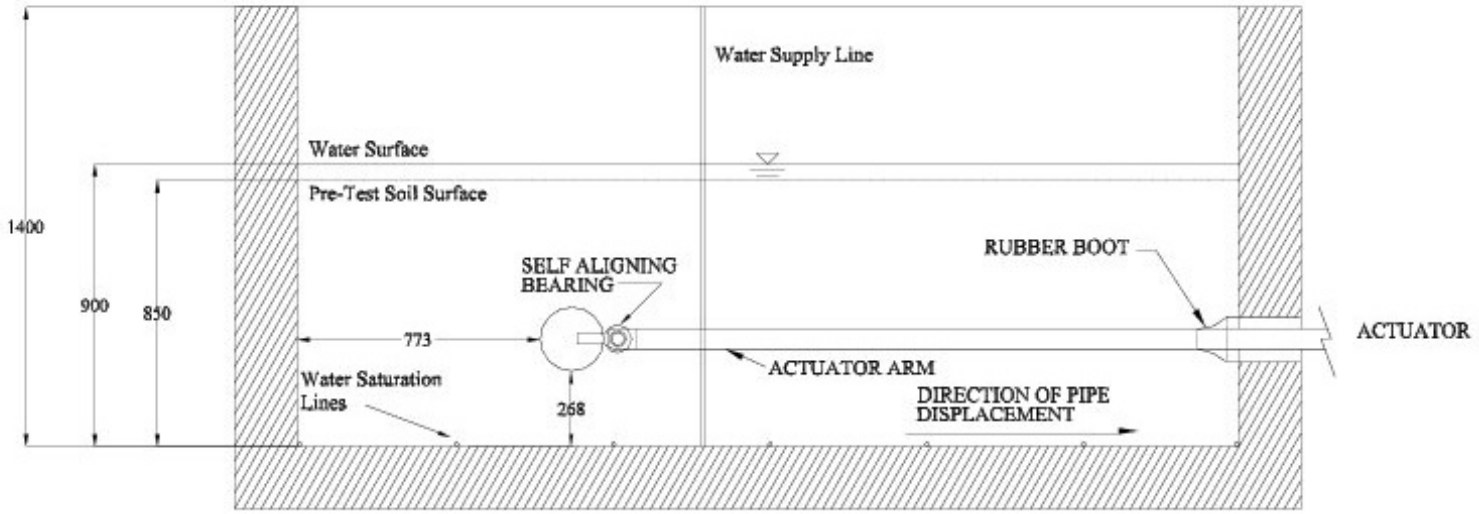

Figure 2 Experimental set-up of test MMS02R – cross-section

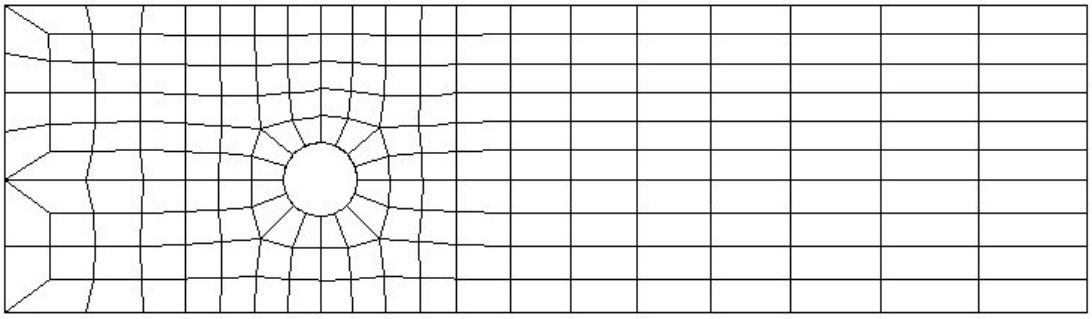

Figure 3 Finite element mesh for back-analysis of test MMS02R

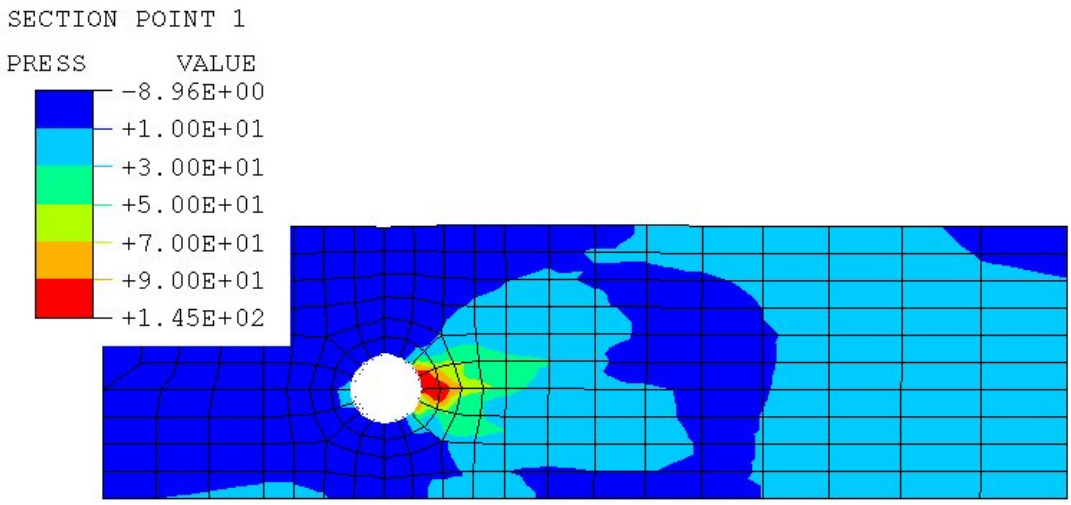

Figure 4 Contours of mean effective stress, p (kPa) – back-analysis of test MMS01

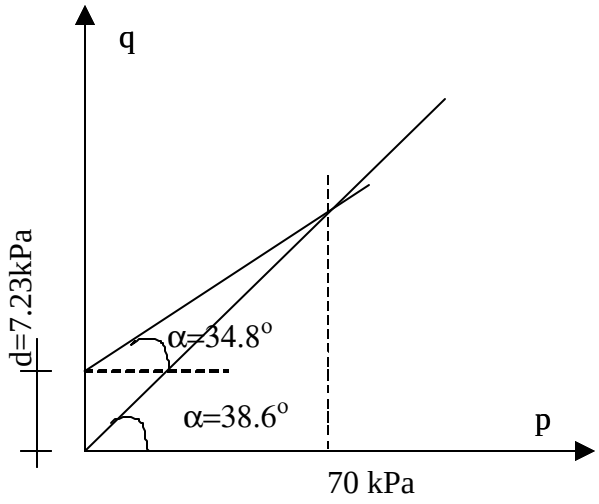

Figure 5 Friction angle and cohesion in the *p*-*q* plane for dense sand

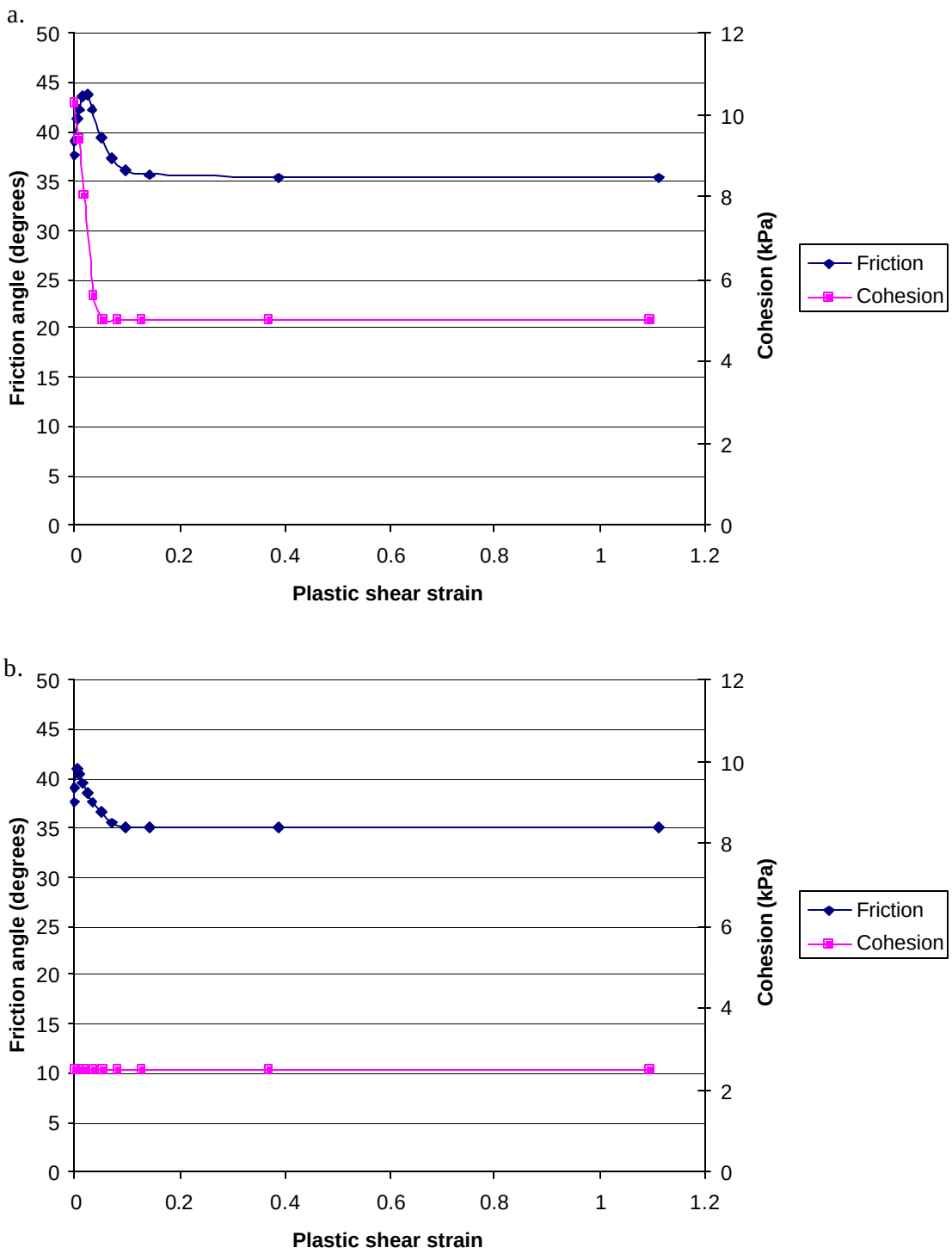

Figure 6 Hardening/softening rules: (a) MMS01 sand with relative density of 95%; and (b) MMS02R sand with relative density of 66%

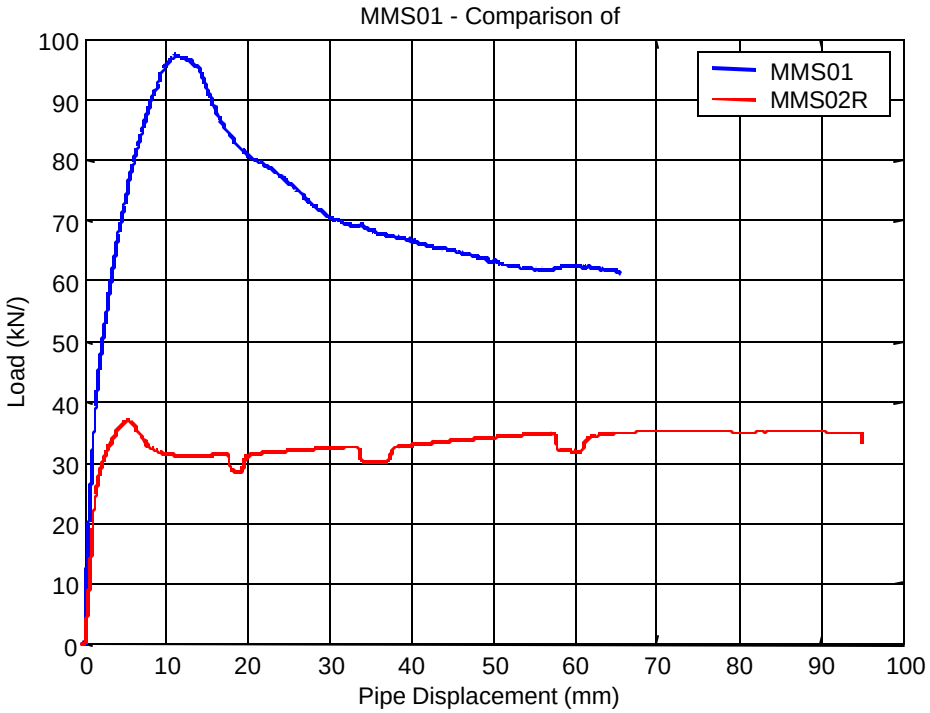

Figure 7 Comparison of MMS01 and MMS02R load-displacement curve (experimental results in terms of total pull force per 3m of pipe)

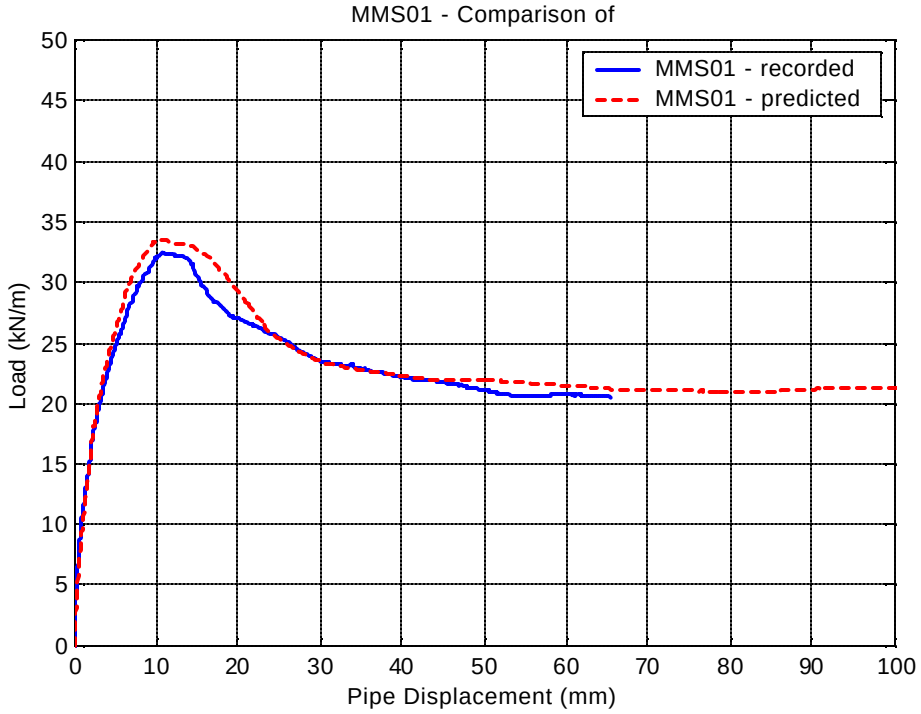

Figure 8 Test MMS01 - Comparison of predicted and recorded force displacement curves for dense dry sand

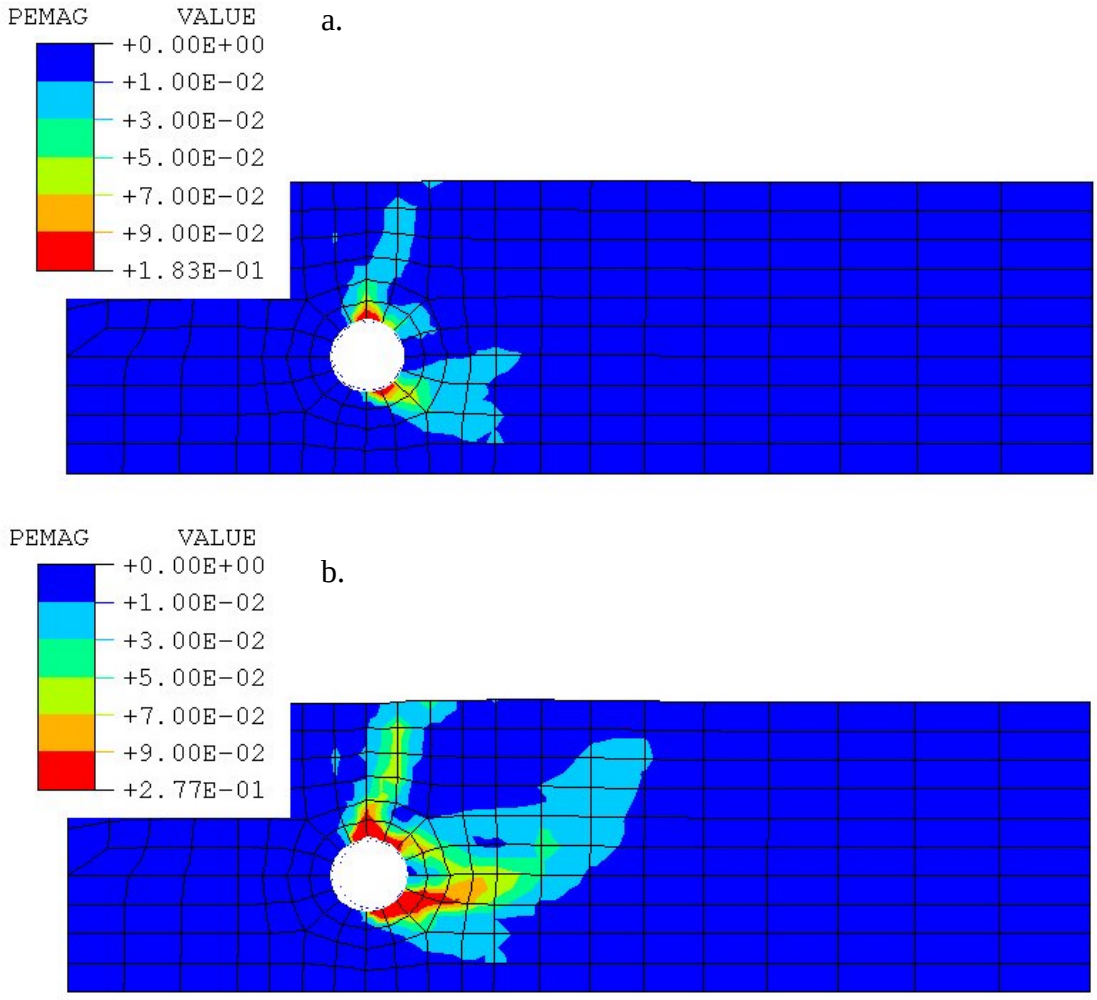

Figure 9 Predicted contours of plastic shear strain (pemag) for test MMS01: (a) pipe displacement = 10 mm and (b) pipe displacement = 20 mm

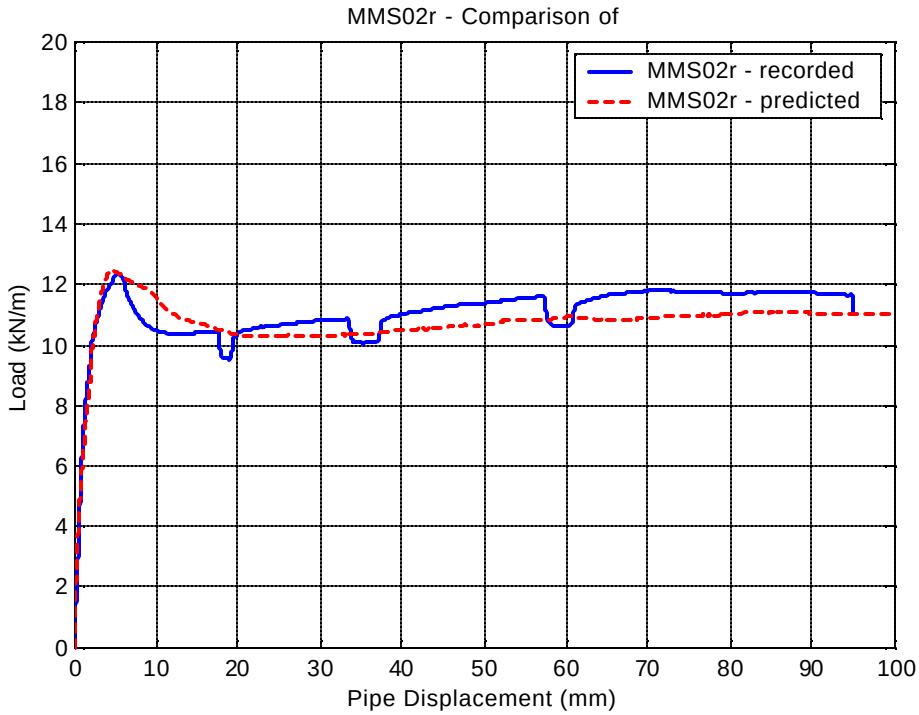

Figure 10 Comparison of predicted and recorded force displacement curves for medium dense saturated sand– test MMS02R

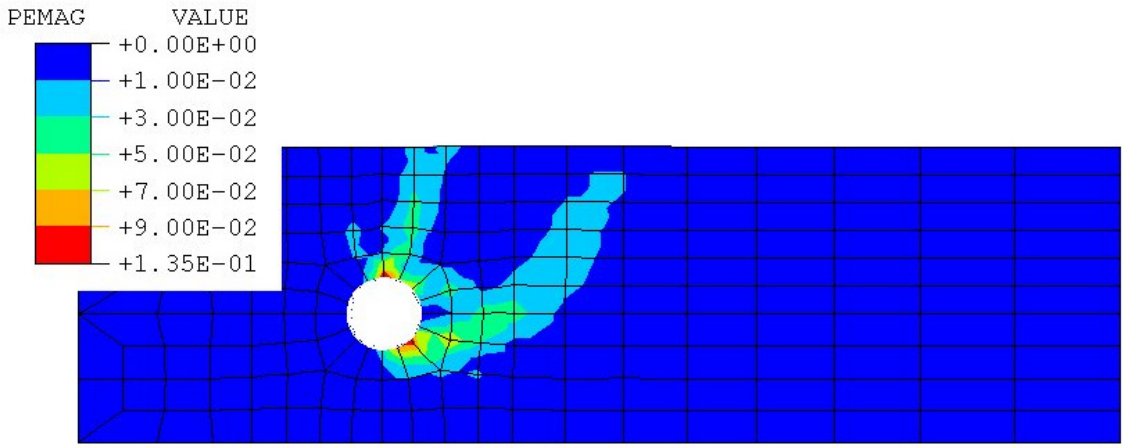

Figure 11 Predicted contours of plastic shear strain (pemag) at pipe displacement = 10 mm - test MMS02R

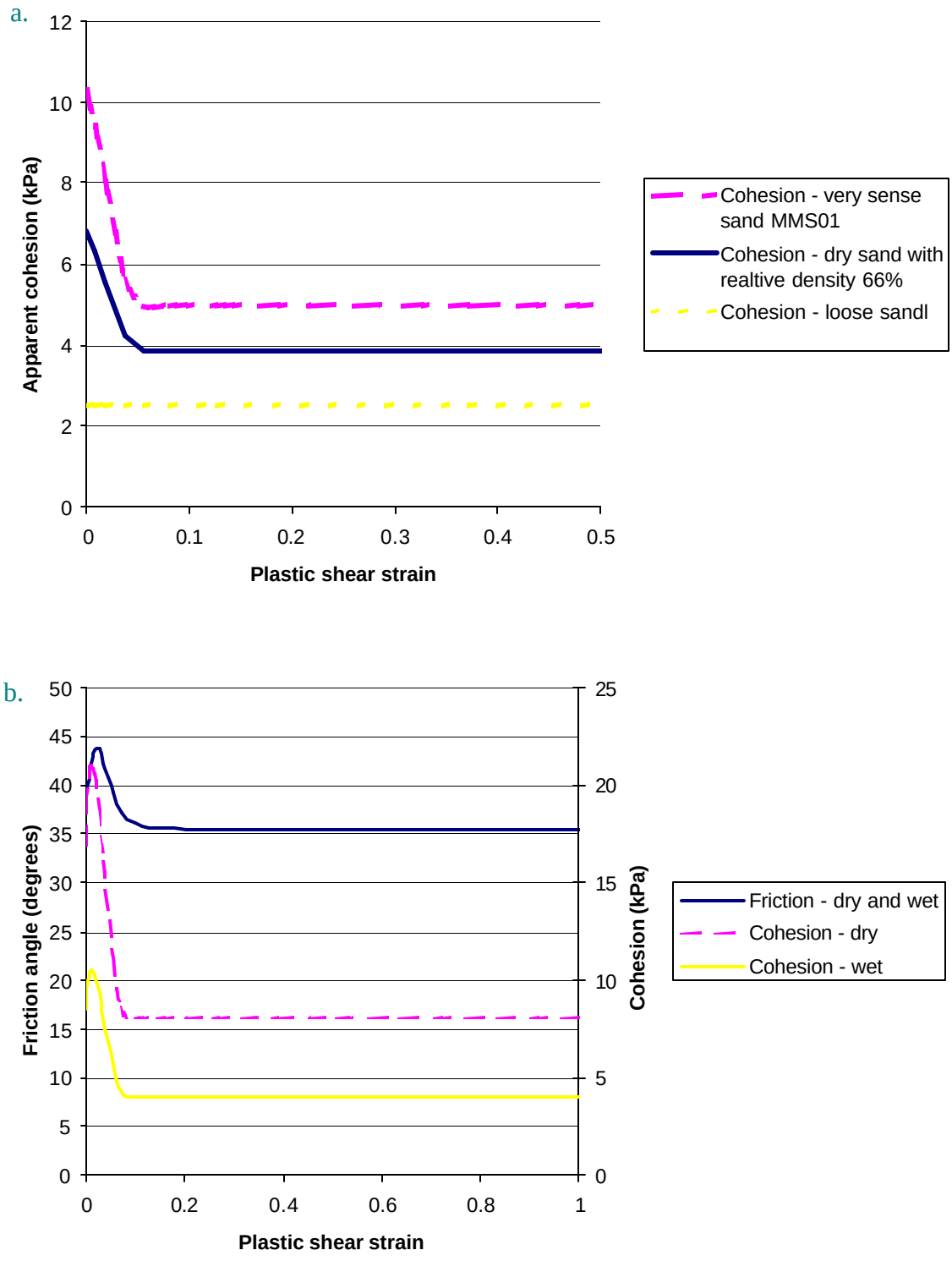

Figure 12 Variation of apparent cohesion: (a) estimation of apparent cohesion for dry sand with relative density of 66%; (b) estimated cohesion for a saturated soil corresponding to the GSC tests with dense sand (Hurley et al., 1998a&b) – yellow line.

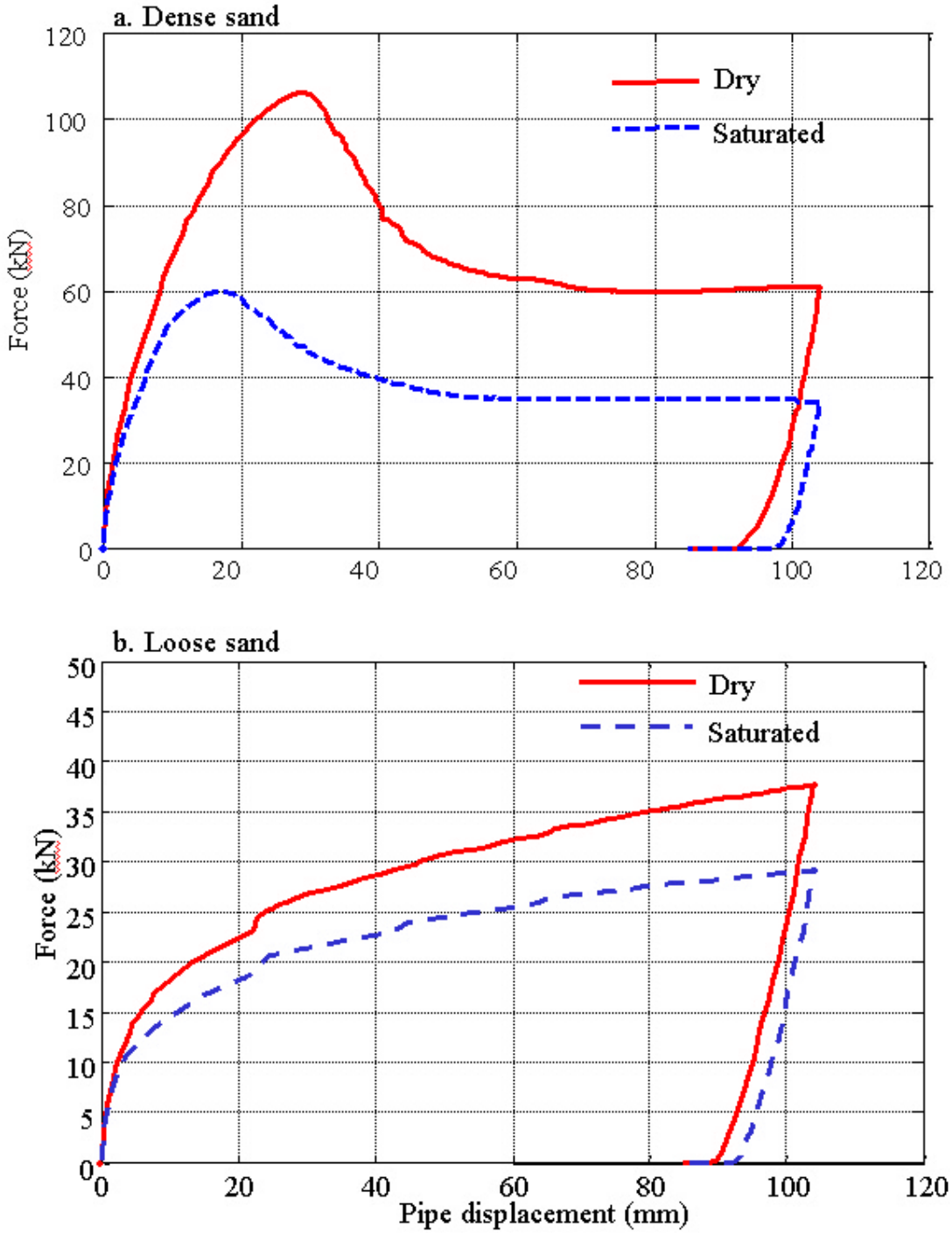

Figure 13 Predicted effects of saturation on force-displacement curves in large scale tests of lateral loading of a rigid pipe in sand (the curves for dry sand are from Figure 2.13 of Popescu et al. 2001)

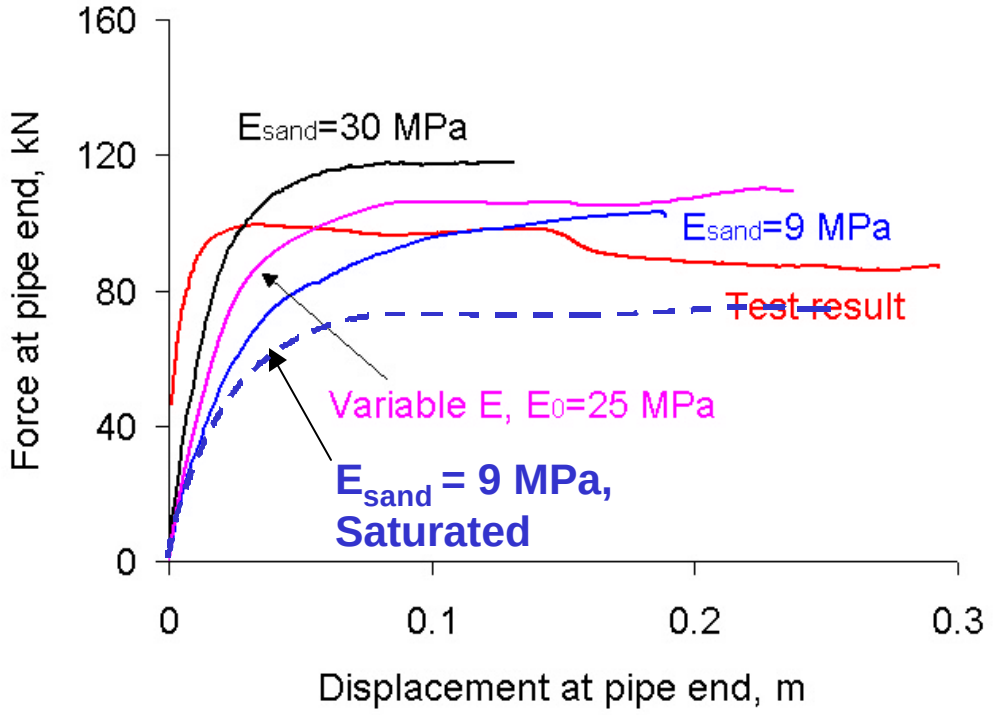

Figure 14 Effects of saturation on the force-displacement curves for a flexible pipe buried in dense sand subjected to moment loading (test GSC01) – dashed, blue line

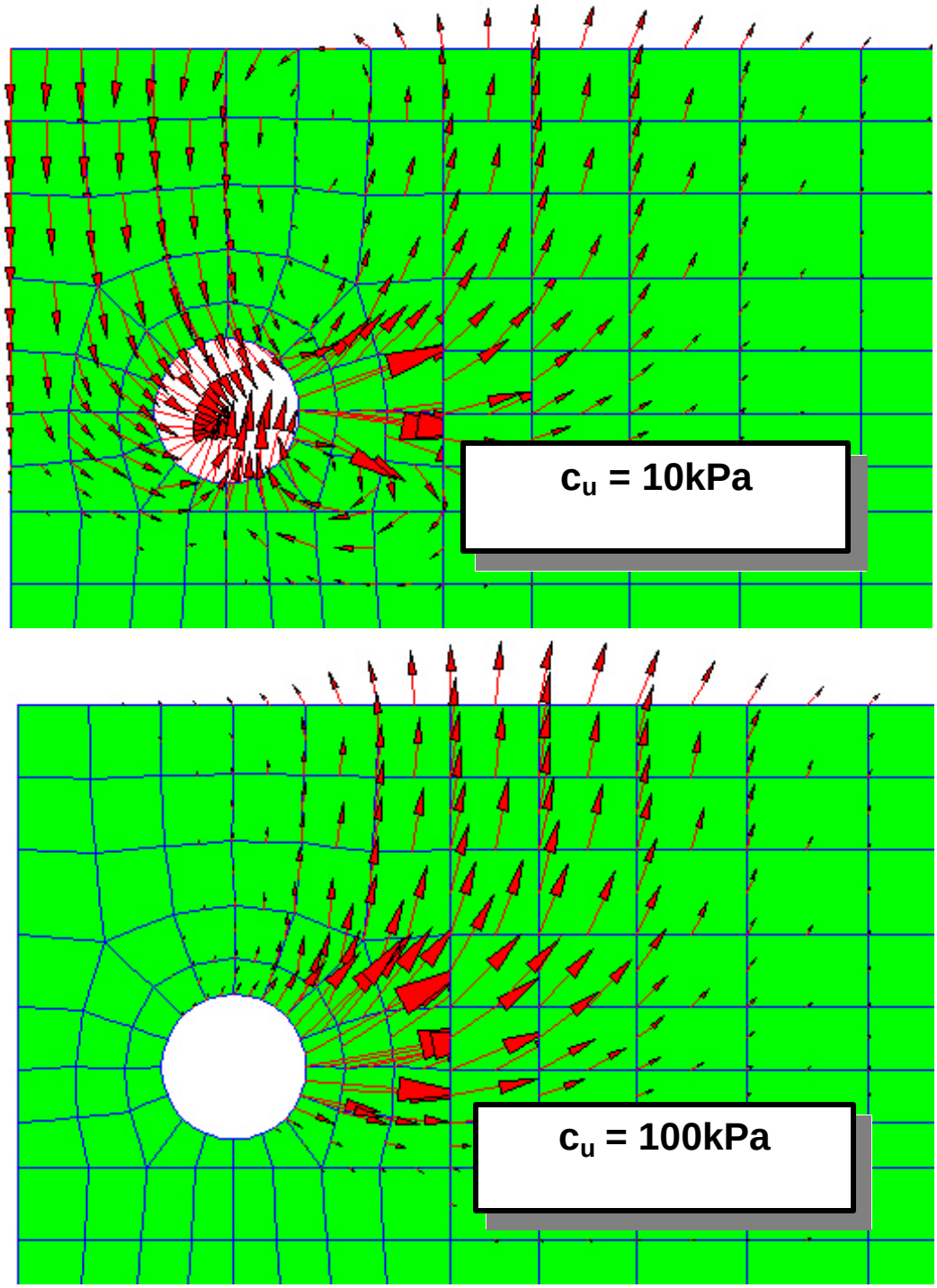

Figure 15 Lateral loading of a rigid pipe in clay: predicted failure mechanisms for different undrained shear strengths of the soil

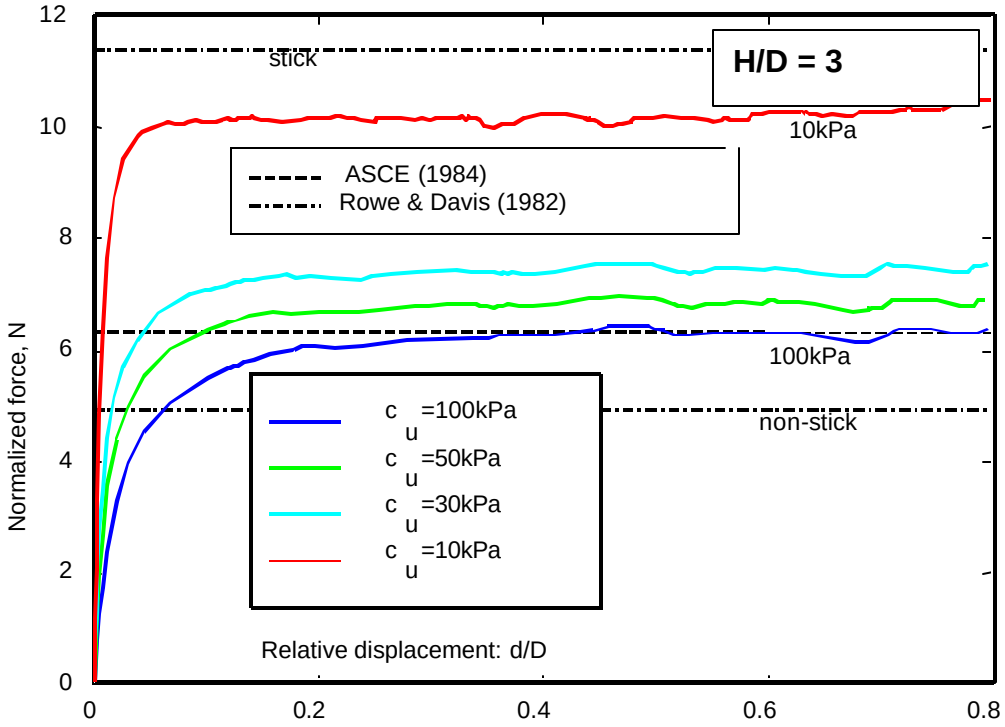

Figure 16 Predicted and recommended interaction forces for lateral loading of a rigid pipe in clay

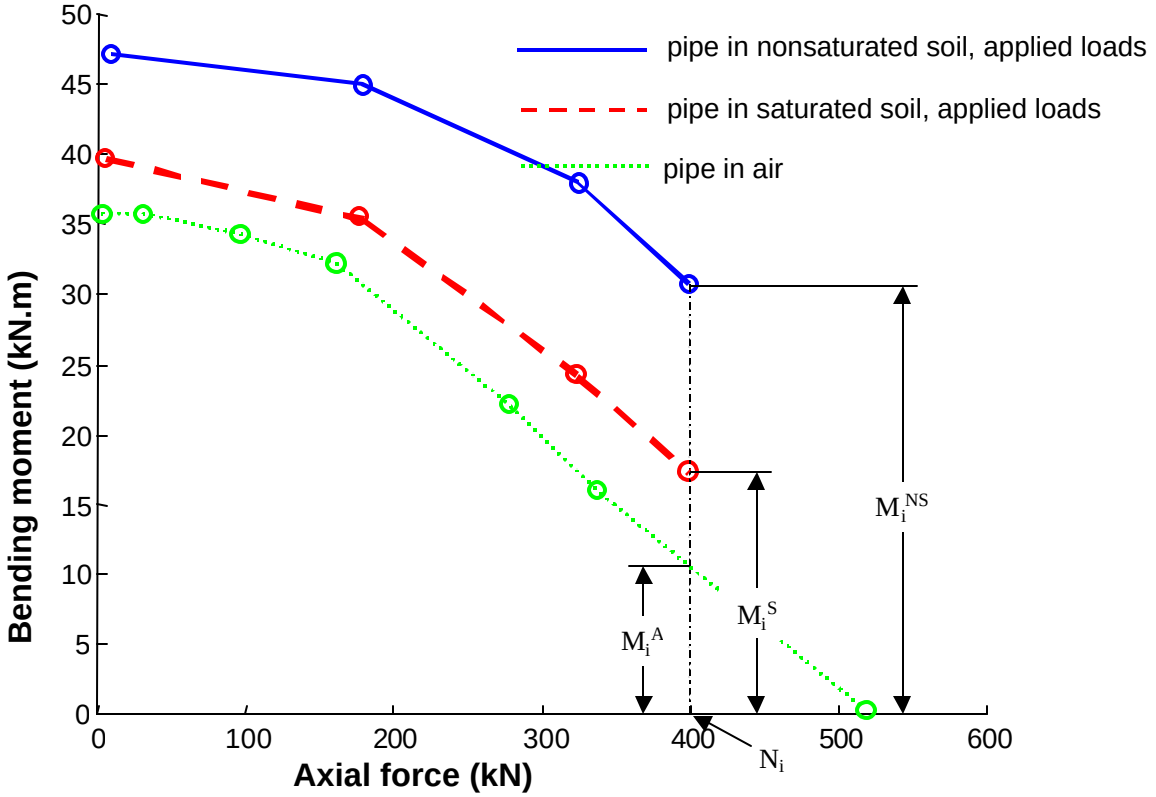

Figure 17 Estimated interaction diagram for a pipe in saturated clay (red, dashed line)